JOURNAL OF SPACECRAFT AND ROCKETS
Vol. 42, No. 5, September–October 2005

Tundra Constellation Design and Stationkeeping

Michael J. Bruno*
San José State University, San José, California 95192
and
Henry J. Pernicka†
University of Missouri–Rolla, Rolla, Missouri 65409-0050

Constellations of satellites in Tundra orbits provide an innovative alternative to the increasingly crowded geostationary orbit belt. The Tundra constellation uses three or more spacecraft in inclined geosynchronous orbits. The nominal orbit design for the constellation must minimize any undesirable perturbation effects to provide affordable stationkeeping costs. We describe a study of the Tundra orbit regime and design of constellations given a sample set of basic constraints. Frozen and partially frozen orbits are then sought from which to construct constellations allowing for reduced stationkeeping requirements. Perturbation effects from third-body and geopotential sources are quantified and used to select orbits that will provide the needed coverage while providing a reasonable propellant budget.

Nomenclature

a	=	orbit semimajor axis
a'	=	perturbing body semimajor axis
e	=	orbit eccentricity
e'	=	perturbing body eccentricity
F	=	semimajor axis scaling factor
h	=	semi-equinoctial element
i	=	orbit inclination
i'	=	perturbing body inclination
J_2	=	oblateness geopotential coefficient
k	=	semi-equinoctial element
M	=	orbit mean anomaly
n	=	orbit mean motion
R	=	disturbing potential function
$R_\oplus$	=	radius of the Earth
r	=	radial distance
Δ	=	$\Omega - \Omega'$
ΔV_n	=	normal velocity change
ΔV_r	=	radial velocity change
ΔV_t	=	transverse velocity change
μ	=	gravitational parameter
ν	=	orbit true anomaly
Ω	=	orbit ascending node
Ω'	=	perturbing body ascending node
ω	=	orbit argument of perigee

Introduction

ON 26 July 1963, Syncom 2 became the first geostationary satellite.[1] Since then, hundreds of satellites have been launched into geostationary orbit. Today, there are more than 270 operational satellites occupying geostationary orbit. Most of these satellites are built to operate for more than a decade, and construction of more new satellites continues. As a result, the available space to place new satellites is growing sparse. In response to the increasing difficulty in obtaining orbital slots in geostationary orbit, some innovative companies are breaking away from the geosatellite "mold" and are using constellations of satellites in inclined, eccentric, geosynchronous orbits, known as "Tundra" orbits, from which to distribute their services.

The Tundra orbit constellation is a relatively new idea in the commercial satellite world.[2] To date, Sirius Satellite Radio, Inc., is the only commercial company operating satellites in this regime.[3] To increase the commercial viability of this type of constellation, a constellation design method that reduces the propellant required for orbit maintenance while providing the needed communications coverage is desirable.

There has only been limited study of this regime to date. Turner[4] discusses several commercial uses for Tundra orbits, whereas an alternative to the use of Tundra orbits was proposed in two related efforts,[5,6] which examined the use of 8-h orbits near the critical inclination in constellation design to provide communication services to northern latitudes. Dufour[7] used Walker's coverage analysis to consider the use of elliptical orbits to provide zonal coverage. These various constellations provide good coverage, but might require the spacecraft to pass through high-radiation environments repeatedly. Another study[8] briefly considered the use of inclined and eccentric doubly geosynchronous orbits for Earth observation. Although these efforts mainly discussed the applications of such orbits, only one early stationkeeping strategy was proposed.[9] However, the third-body effects of solar and lunar gravity were not addressed and can perturb an actual constellation into a less useful form. The current study shows that these third-body perturbations significantly influence these orbits. The study of their effects helps determine an effective way to reduce stationkeeping requirements.

In any constellation design, an effective way to reduce stationkeeping propellant is to reduce the number of orbit parameters requiring correction. This can either be achieved by allowing large tolerances on specific elements or by identifying a nominal orbit that is "frozen," such that one or more elements do not vary greatly over time. The former is usually not a practical solution because the payload will typically require substantially smaller tolerances than would otherwise occur naturally. Frozen orbits, however, are routinely used in operations today. A constellation of frozen or nearly frozen orbits could be used to realize propellant savings for constellation operators. The open literature contains numerous works that involve frozen orbits, including Refs. 10 and 11 that identify a variety of frozen orbits for different applications. Many of these studies do not apply to orbits with higher levels of eccentricity as is used in the current study, or examine the effects of third-body perturbations to the frozen nature of an orbit.

Received 20 January 2004; revision received 17 August 2004; accepted for publication 20 August 2004.

*Graduate Student; current address: 4921 Mansbury Street, Fremont, CA 94538; mike.bruno@comcast.net. Senior Member AIAA.

†Associate Professor, Mechanical and Aerospace Engineering, 122A ME Annex, 1870 Miner Circle; pernicka@umr.edu. Senior Member AIAA.

A four-step process is used to achieve a constellation design process providing reduced stationkeeping requirements. First, a numerical survey of the orbit regime is performed to characterize the behavior of these orbits. This will verify that frozen orbits exist and allow for the validation of assumptions used to simplify analytical and numerical modeling. Second is an analytic approach for identifying frozen orbits. Although the numerical survey provides a rough approximation of the initial conditions for frozen orbits, an analytic approach to determining the best initial conditions is desirable. The third is constellation design, which can be assembled using frozen and partially frozen (discussed in detail later) orbits. Last is a quantitative evaluation of the stationkeeping requirements as well as the evaluation of various performance metrics of the constellation.

Tundra Orbit Constellations

A Tundra orbit is not any single orbit; rather, it is an orbit with specific characteristics. A Tundra orbit is characterized first by a geosynchronous period. The second key feature of a Tundra orbit is nonzero inclination. The nonzero inclination allows the satellite to travel into the northern and southern hemispheres. Lastly, a nonzero orbital eccentricity coupled with an argument of perigee equal to either 270 or 90 deg results in the satellite spending more time in the northern or southern hemisphere, respectively.

This type of orbit has many attractive features to a commercial operator. The geosynchronous period of the orbit allows each satellite to maintain its position over the same region of the world allowing operators to tailor their services to a specific market region. The higher inclinations allow the satellite to broadcast with higher elevation angles into that desired region. As the satellite travels into the higher latitudes, the signals are received on the ground from overhead rather than from a low elevation angle. This feature mitigates the "urban jungle" effect in large cities as well as providing coverage into remote mountainous or heavily forested regions. A nonzero eccentricity coupled with an argument of perigee near 90 or 270 deg also allows the satellite to spend more time over the desired hemisphere, subsequently increasing the time the satellite spends over the desired region. An example ground trace of a Tundra orbit is shown in Fig. 1.

To provide continuous around-the-clock coverage to a region, a group of satellites in similar orbits is required. Because a satellite passes above and below the equator during each orbit, a portion of the orbit is not usable for service delivery. This unusable portion is defined as those times in the orbit when the elevation angle to the coverage area is less than zero (although a 5-deg "mask" was used in this study to account for ground interference from mountains, buildings, etc.). In the case of Fig. 1, this unusable region corresponds roughly to the area below the equator (when targeting coverage to the northern hemisphere). Thus, the minimum number of satellites

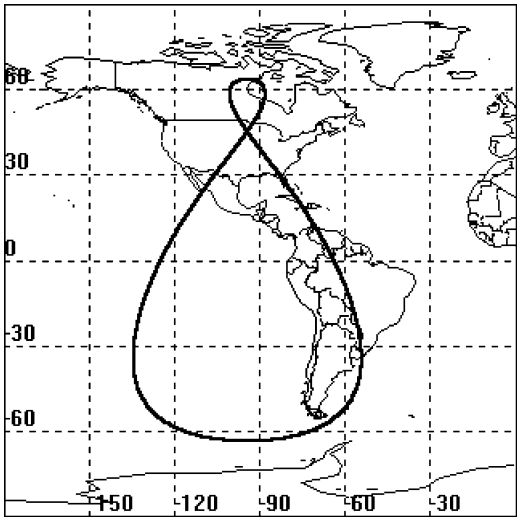

Fig. 1 Tundra orbit ground trace.

Table 1 Baseline orbital elements

Parameter	Value
Semimajor axis a, km	42,164.16
Inclination i, deg	63.4
Eccentricity e	0.2684
Argument of perigee ω, deg	270
Right ascension of the ascending node Ω, deg	30, 150, 270

required to provide around-the-clock coverage of a region is simply the integer number of satellites required such that sum of their coverage time is greater than 24 h per day. However, this only provides the number of satellites for continuous coverage. Because one of the benefits of a Tundra orbit is high elevation angle coverage, it follows that the more satellites there are in the constellation the higher the average elevation angle will be.

As a basis for this study, a baseline constellation of three orbits was selected. These orbits provide a foundation from which to gauge the relative benefit of one orbit vs another. The orbital elements of these baseline orbits are shown in Table 1. The semimajor axis corresponds to a geosynchronous orbital period. The inclination, set to the critical value to reduce perigee drift, allows the satellite to rise to higher latitudes, where a majority of the population centers around the world are located. The nonzero eccentricity causes the satellite to pass through different portions of the orbit at different rates. The baseline eccentricity roughly splits each orbit into three 8-h blocks, from ascending node to apogee, apogee to descending node, and from descending node through perigee and back to the ascending node. The argument of perigee is chosen to place apogee in the northern hemisphere. The ascending nodes were arbitrarily selected to define three evenly spaced orbit planes to provide a constellation of satellites in which at least two satellites will always be above the equator, capable of delivering services to a designated region. Last, the mean anomaly is time and date dependent and together with the ascending node defines the area over which the satellite orbits Earth.

Tundra Orbit Behavior

To date, Tundra orbits have not yet been used significantly, and thus there is not a great volume of data or analyses in the open literature concerning the behavior of satellites in such orbits. Thus, it is insightful to perform numerical simulations of the orbit regime to determine the general behavior of these orbits under the influence of various perturbations. The most significant perturbative accelerations were examined: Earth's geopotential, solar and lunar gravity. (Drag and solar radiation pressure were shown to have negligible effect on Tundra orbits.[12])

To show how the range of orbits behaves, a series of one-year simulations were performed using the orbit propagator POHOP developed by the Jet Propulsion Laboratory, California Institute of Technology. This propagator is useful for these studies because it allows all of the perturbations of interest to be modeled either independently or in combination. Along with the solar and lunar gravitation, these simulations used the GEMT2 Earth gravity field model of degree eight and order eight. The initial conditions of the simulations were varied in ascending node and inclination: ascending node was varied from 30 to 360 deg at 30-deg intervals, and inclination varied from 30 to 70 deg at 10-deg intervals.

The results of the simulations are presented as contour plots in Figs. 2a–2d. The ascending node is shown along the abscissa, while inclination is depicted along the ordinate. The shading of the contour illustrates the magnitude of deviation from the initial condition after one year. More detailed results can be found in Refs. 12 and 13.

It can be seen in Figs. 2a–2d that all of the orbital elements, except for the ascending node, have regions where their yearly deviations are quite small. Of particular interest is the argument of perigee. For all values of ascending node, there is a corresponding value of inclination that should ostensibly freeze the perigee point. This has the potential to create significant propellant savings because the

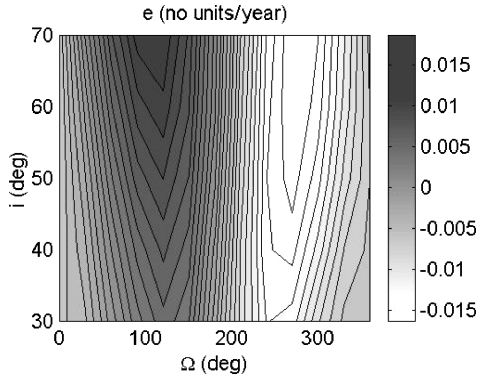

Fig. 2a Eccentricity deviation caused by solar, lunar, and geopotential perturbations.

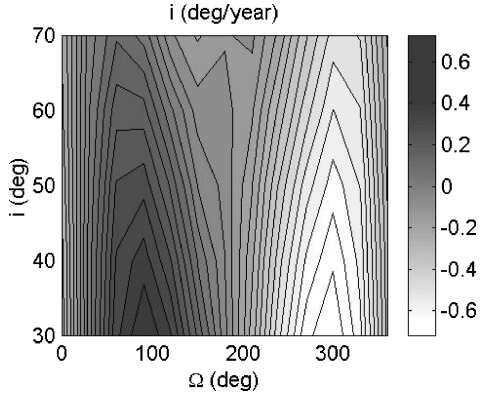

Fig. 2b Inclination deviation caused by solar, lunar, and geopotential perturbations.

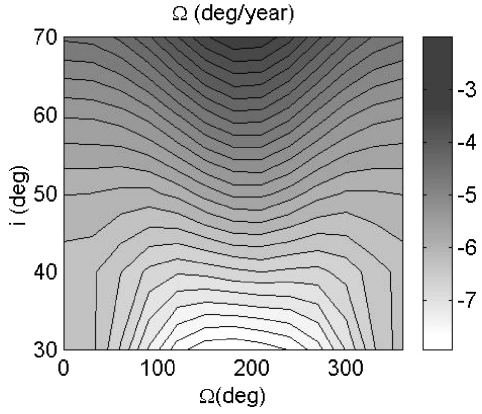

Fig. 2c Ascending node deviation caused by solar, lunar, and geopotential perturbations.

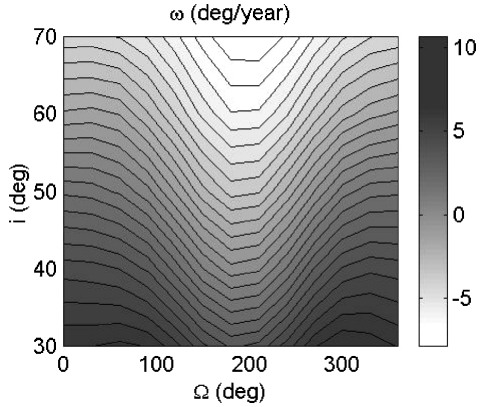

Fig. 2d Argument of perigee deviation caused by solar, lunar, and geopotential perturbations.

argument of perigee can be costly to correct in large, high-energy orbits such as the Tundra type. Inclination and eccentricity also have regions of low variation that correlate to the value of the ascending node. These simulations show that there are initial orbit conditions that will likely allow eccentricity, inclination and/or the argument of perigee to be frozen.

Seeking Frozen Orbits

The results presented in the preceding section provide a rough numerical assessment of the effects of the most significant perturbations for a Tundra-type orbit. However, a method by which to identify specific orbital elements for the orbits of the constellation needs to be provided. To reduce stationkeeping costs, a frozen or near-frozen orbit that minimizes the changes to eccentricity and argument of perigee is sought.

The gravitational forces of the Earth, sun, and moon are the primary perturbations affecting these orbits. A model was sought that would include these effects yet be simple enough to allow the analytic identification of frozen orbits. The open literature contains many works that address the effects of third-body perturbations. Those by Broucke[14] and Cefola[15] are noteworthy here, because they address long-term third-body effects, and Ref. 15 provides a good survey of literature related to third-body effects. Kwok[16] presents a doubly averaged potential function for third-body perturbations expressed in planet–equator coordinates. Using planet–equator coordinates allows the third-body potential to be easily added to the geopotential function. To eliminate the singularity when eccentricity is zero, Kwok uses semi-equinoctial elements h and k with

$$h = e\sin(\omega) \tag{1}$$

$$k = e\cos(\omega) \tag{2}$$

The remaining classical orbital elements semimajor axis a, inclination i, and right ascension of the ascending node (Ω) are then used with h and k. The needed equations of motion[16] using the semi-equinoctial elements are

$$\frac{\mathrm{d}h}{\mathrm{d}t} = \frac{\sqrt{1-e^2}}{na^2}\frac{\partial R}{\partial k} - \frac{k\cot i}{na^2\sqrt{1-e^2}}\frac{\partial R}{\partial i} \tag{3}$$

$$\frac{\mathrm{d}k}{\mathrm{d}t} = -\frac{\sqrt{1-e^2}}{na^2}\frac{\partial R}{\partial h} + \frac{h\cot i}{na^2\sqrt{1-e^2}}\frac{\partial R}{\partial i} \tag{4}$$

$$\frac{\mathrm{d}i}{\mathrm{d}t} = \frac{\cot i}{na^2\sqrt{1-e^2}}\left(k\frac{\partial R}{\partial h} - h\frac{\partial R}{\partial k}\right) - \frac{1}{na^2\sqrt{1-e^2}\sin i}\frac{\partial R}{\partial \Omega} \tag{5}$$

$$\frac{\mathrm{d}\Omega}{\mathrm{d}t} = \frac{1}{na^2\sqrt{1-e^2}\sin i}\frac{\partial R}{\partial i} \tag{6}$$

This function, as a result of the doubly averaged third-body perturbation, is given by Kwok as

$$\begin{aligned} R = {} & (\mu'/a')(a/a')^2\left[1/(1-e'^2)^{\frac{3}{2}}\right]\left(\left(\tfrac{3}{4}\sin^2 i' - \tfrac{1}{2}\right)\right. \\ & \times\left[\tfrac{3}{4}\sin^2 i(1-k^2+h^2) - \tfrac{1}{2}\left(1+\tfrac{3}{4}k^2+\tfrac{3}{4}h^2\right)\right] \\ & + \tfrac{3}{8}\sin 2i'\left[5kh\sin\Delta\sin i + \tfrac{1}{2}\sin 2i\cos\Delta(1-k^2+4h^2)\right] \\ & + \tfrac{3}{8}\sin 2i'\left\{\tfrac{1}{2}\cos 2\Delta[5(k^2-h^2)+\sin^2 i(1-k^2+4h^2)]\right. \\ & \left.\left. - 5kh\cos i\sin 2\Delta\right\}\right) \end{aligned} \tag{7}$$

where the variables with primes refer to the perturbing body and μ' is the gravitational parameter of the perturbing body. This expanded

potential has been averaged over the mean anomaly of both the spacecraft orbit and the perturbing body, then truncated at first order. Thus, an implicit assumption is that the orbital elements of the spacecraft vary slowly during one orbit of the perturbing body. The partial derivatives needed by the equations of motion in Eqs. (3–6) are then

$$\frac{\partial R}{\partial h} = \frac{\mu'}{a'}\left(\frac{a}{a'}\right)^2 \frac{1}{(1-e'^2)^{\frac{3}{2}}}\left\{\frac{3}{2}h\left(\frac{3}{4}\sin^2 i' - \frac{1}{2}\right)(4\sin^2 i - 1) + \frac{3}{8}\sin 2i' \sin i\,(5k\sin\Delta + 8h\cos i\cos\Delta) - \frac{3}{8}\sin^2 i'[h\cos 2\Delta(1+4\cos^2 i) + 5k\cos i\sin 2\Delta]\right\} \tag{8}$$

$$\frac{\partial R}{\partial k} = \frac{\mu'}{a'}\left(\frac{a}{a'}\right)^2 \frac{1}{(1-e'^2)^{\frac{3}{2}}}\left\{-\frac{3}{2}k\left(\frac{3}{4}\sin^2 i' - \frac{1}{2}\right)(\sin^2 i + 1) + \frac{3}{8}\sin 2i' \sin i\,(5h\sin\Delta + 2k\cos i\cos\Delta) + \frac{3}{8}\sin^2 i'[k\cos 2\Delta(4+\cos^2 i) - 5h\cos i\sin 2\Delta]\right\} \tag{9}$$

$$\frac{\partial R}{\partial i} = \frac{\mu'}{a'}\left(\frac{a}{a'}\right)^2 \frac{1}{(1-e'^2)^{\frac{3}{2}}}\left\{\left(\frac{3}{4}\sin^2 i' - \frac{1}{2}\right) \times \left[\frac{3}{2}\sin i\cos i(1-k^2+4h^2)\right] + \frac{3}{8}\sin 2i'[(2\cos^2 i - 1)\cos\Delta(1-k^2+4h^2) + 5kh\cos i\sin\Delta] + \frac{3}{8}\sin 2i'[\sin i\cos i(1-k^2+4h^2)\cos 2\Delta + 5kh\sin i\sin 2\Delta]\right\} \tag{10}$$

$$\frac{\partial R}{\partial \Omega} = \frac{\mu'}{a'}\left(\frac{a}{a'}\right)^2 \frac{1}{(1-e'^2)^{\frac{3}{2}}}\left\{\frac{3}{8}\sin 2i' \sin i[5kh\cos\Delta - \cos i\sin\Delta(1-k^2+4h^2)] - \frac{3}{8}\sin^2 i'\sin 2\Delta[(1-h^2+4k^2) - \cos 2i(1-k^2+4h^2)] - \frac{15kh}{4}\sin^2 i'\cos i\cos 2\Delta\right\} \tag{11}$$

These are summed with the potential derivatives due to J_2 (higher-order geopotential terms can also be similarly added) to the equations of motion. The disturbing potential derivatives due to J_2 only are

$$\frac{\partial R}{\partial h} = \frac{3}{2}\mu J_2 \frac{R_\oplus^2}{a^3}\frac{1-(3/2)\sin^2 i}{(1-e^2)^{\frac{5}{2}}}h \tag{12}$$

$$\frac{\partial R}{\partial k} = \frac{3}{2}\mu J_2 \frac{R_\oplus^2}{a^3}\frac{1-(3/2)\sin^2 i}{(1-e^2)^{\frac{5}{2}}}k \tag{13}$$

$$\frac{\partial R}{\partial i} = -\frac{3}{2}\mu J_2 \frac{R_\oplus^2}{a^3}\frac{\sin i\cos i}{(1-e^2)^{\frac{3}{2}}}h \tag{14}$$

$$\frac{\partial R}{\partial \Omega} = 0 \tag{15}$$

With this model available in the convenient reference of Earth's equatorial plane, attention is turned to seeking frozen orbits. The approach begins by fixing the semimajor axis at the geosynchronous value (42,164.16 km) and the argument of perigee at 270 deg. Then eccentricity, inclination, and right ascension of the ascending node were varied from their baseline values in Table 1 to seek frozen orbits. In particular, orbits were sought such that eccentricity and argument of perigee are frozen, or at least vary slowly so that they might be easily controlled with stationkeeping. In the semi-equinoctial elements, the frozen orbit requirement is then

$$\frac{\mathrm{d}h}{\mathrm{d}t} = 0 \tag{16}$$

$$\frac{\mathrm{d}k}{\mathrm{d}t} = 0 \tag{17}$$

Because the argument of perigee $\omega = 270$ deg, then $h = -e$, and $k = 0$. The equations of motion (3) and (4) then simplify to

$$\frac{\mathrm{d}h}{\mathrm{d}t} = \frac{\sqrt{1-e^2}}{na^2}\frac{\partial R}{\partial k} \tag{18}$$

$$\frac{\mathrm{d}k}{\mathrm{d}t} = -\frac{\sqrt{1-e^2}}{na^2}\frac{\partial R}{\partial h} - \frac{e\cot i}{na^2\sqrt{1-e^2}}\frac{\partial R}{\partial i} \tag{19}$$

Setting Eqs. (18) and (19) to zero in an attempt to freeze the orbit requires that

$$\frac{\partial R}{\partial k} = 0 \tag{20}$$

$$(1-e^2)\frac{\partial R}{\partial h} + e\cot i\frac{\partial R}{\partial i} = 0 \tag{21}$$

The MATLAB® function "fmins" was used to minimize the rss value of Eqs. (20) and (21) using the baseline elements of Table 1 as initial values. At the end of the search by fmins, the rss was very small (3.5072×10^{-9}) and effectively zero. Thus, roots were found that satisfy Eqs. (20) and (21) and are shown in Table 2. Note that these values correspond to regions of small variances in Fig. 2, as expected.

To test whether these "improved" elements actually froze the orbit, additional simulations were run. A simulation was run that tested the improved orbit using a more realistic perturbation environment. The geopotential model was expanded to 42×42, and drag and solar radiation pressure were included. (Arbitrary but typical satellite characteristics were used: mass = 2000 kg, area = 75 m^2, and drag coefficient = 2.0.) Figures 3a–3d show that the "improved" elements do reduce the drift rate of eccentricity and argument of perigee. Although not truly frozen, the orbit behavior is clearly improved. Thus the improved orbital elements should provide a practical nominal orbit for use in a Tundra constellation.

Note that a previous study[12] showed that over a one-year period drag and solar radiation pressure had negligible effect (although increased values of spacecraft cross-section area from larger solar panels and antennas were not specifically considered and could lead to significant perturbative effects). Reference 13 also includes a comparison of the results shown in Fig. 3 to a simulation in which solar radiation pressure and drag were omitted, showing nearly identical element histories. Thus for the baseline parameters used in this study, drag and solar radiation pressure are not of prime concern in the constellation design.

Table 2 Frozen orbit algorithm results

Parameter	Initial value	Solved value
Inclination i, deg	63.5	62.314
Eccentricity e	0.2684	0.3440
Argument of perigee ω, deg	270	270
Right ascension of the ascending node Ω, deg	30	8.666

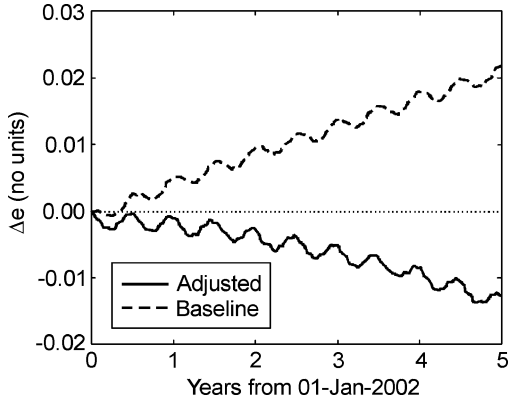

Fig. 3a Search results, all perturbations acting: eccentricity.

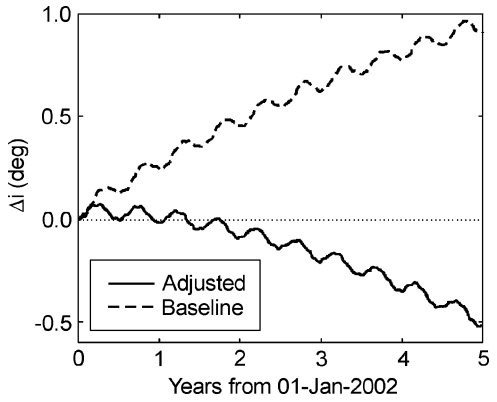

Fig. 3b Search results, all perturbations acting: inclination.

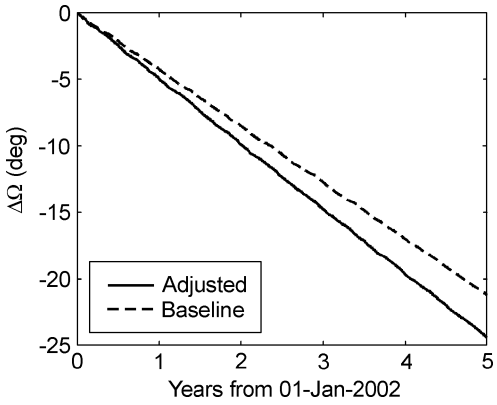

Fig. 3c Search results, all perturbations acting: ascending node.

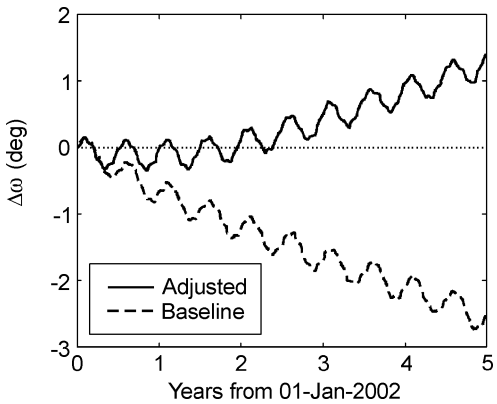

Fig. 3d Search results, all perturbations acting: argument of perigee.

Constellation Design

Tundra constellations have many possible configurations, typically ranging from three to six satellites. A three-satellite configuration was arbitrarily chosen for this initial study. All orbits were chosen as geosynchronous, with inclinations above 30 deg and nonzero eccentricity. This combination of elements allows the constellation to provide the benefits mentioned in the Introduction.

Part of the nominal orbit design process is defining the operational requirements of the constellation. A Tundra constellation would likely be used to provide a telecommunications service to one of the major population centers of the world. A majority of these centers are located in the northern hemisphere at latitudes greater than 30 deg and less than 70 deg. Thus the argument of perigee of each orbit must be near 270 deg and the inclination constrained to a region between 30 and 70 deg to provide an orbit with apogee over desired regions.

Another key consideration is the duration of time the satellite is in view of its customers. If the eccentricity is too small, the satellite will not provide coverage for a sufficient period of time because the apogee loiter time will be too short. Alternately, if eccentricity is too large, the satellite will cross into the Van Allen radiation belts. Thus, the eccentricity is constrained to values roughly between 0.13 and 0.50. These selections correspond to a 14-h dwell time near apogee and a perigee height just above the outer Van Allen belt (the high proton region, in particular), respectively.[17]

Each satellite requires its own unique plane, and, to maintain proper phasing, they must be separated by 360 deg/n, where n is the number of satellites in the constellation. For simplicity, the ascending node of the first satellite defines the ascending node for the remaining satellites in the constellation by subsequently adding 360 deg/n for each satellite. The parameter ranges defined as allowable are summarized in Table 3.

Nearly Frozen Orbits

With the allowable constellation parameters defined, frozen or nearly frozen orbits are sought that have orbital elements within the ranges defined in Table 3 but that still meet mission objectives. The orbits used for the constellation are selected in a two-step process. The first step is to use the analytic equations (20) and (21) to determine at least one frozen orbit. The second step is to complete the constellation using orbits spaced at the specified ascending node interval, given in Table 3, using orbits that have had the orbit element variations reduced as much as possible, or nearly frozen.

Using the frozen orbit search results in Table 2, the ascending node values of the two companion orbits then become defined at the intervals given in Table 3. Because fmins optimizes the function over all possible values of the ascending node, searching for the companion orbits is further constrained because the remaining ascending node values are then fixed. A constrained, one-dimensional optimizer is used to determine the remaining two companion orbits. In particular, Brent's method[18] is employed to determine values of e and i for the companion orbits.

Because only one variable can be optimized using Brent's method, the best variable to be optimized must be determined. Eccentricity cannot be optimized because it is recognized from Fig. 2 that variation in eccentricity is predominately a function of ascending node, and the ascending nodes for the companion orbits are now fixed.

Table 3 Constellation orbital element allowable ranges

Parameter	Value
Semimajor axis a[a], km	42,164
Inclination i, deg	30–70
Eccentricity e	0.13–0.50
Argument of perigee ω, deg	270
Right ascension of the ascending node Ω, deg	Ω_1, $\Omega_1 + 120$, $\Omega_1 + 240$

[a]The semimajor axis is varied from the value given in Table 1 to better match the rotational rate of the Earth when taking into account the presence of perturbations.

Thus i becomes the best candidate to vary using Brent's method to determine the ideal inclination to minimize the drift in the argument of perigee. The methodology involves stepping through small increments of e while evaluating values of i. When the minimum values of Eqs. (20) and (21) are determined (typically on the order of 10^{-5} km^2/s^2), the result is a nearly frozen companion orbit.

Frozen and nearly frozen orbits were determined to create a three-satellite Tundra orbit constellation. The frozen Tundra constellation elements are shown in Table 4.

To verify the frozen behavior of these orbits, five-year element histories were generated without implementing any corrective maneuvers. Each orbit was propagated using the POHOP orbit propagator with an 8×8 geopotential model as well as with solar and lunar third-body effects. The orbit element histories for each satellite are shown in Figs. 4a–4d.

The initial eccentricity for both companions, satellites 2 and 3, drifted to the minimum allowable eccentricity during the search for nearly frozen orbits. When consulting the results of the orbit regime characterization, this is not surprising. It can be seen in Fig. 2a that for the ascending nodes selected eccentricity variation over time is reduced as the initial value of e correspondingly became smaller.

Constellation Performance

Once a constellation is designed, its ability to perform its mission must be evaluated. In the case of commercial Tundra orbit constellations, the quality of coverage the constellation provides is the highest priority. The key coverage parameter is elevation angle with the best coverage supplied at elevation angles above 60 deg. To evaluate how well the frozen Tundra constellation performs, sample markets of the United States and Europe were examined. These markets were given priority for their commercial marketability; however, the coverage assessment could be applied to any potential market. Representative cities within each region provide a benchmark of coverage quality. The cities evaluated for the two market cases are summarized in Table 5.

To verify the quality of the constellation coverage, elevation angles to various cities were evaluated. To do this, the elevation angle to each satellite over a single day was computed. A Keplerian propagation with no perturbations was executed for each satellite over one orbit. During that orbit, at each time step (10 min), the elevation angle was calculated for the latitude and longitude of each city.

A key component in coverage quality is the mean longitude (the average subsatellite longitude over an orbit); all satellites in the

Table 4 Frozen Tundra constellation elements

Element	Sat 1	Sat 2	Sat 3
a,[a] km	42,158.7	42,153.5	42,153.5
i, deg	62.3136	48.3078	48.0590
e	0.3440	0.1300	0.1300
ω, deg	270	270	270
Ω, deg	8.6657	127	249
M,[b] deg	127.73	322.62	205.88

[a]The semimajor axes were selected such that the mean satellite longitude remained near the desired value for one year.
[b]Epoch of 1 January 2004, 00:00 UT.

Table 5 Representative North American and European cities

City	Latitude, °N	Longitude, °E
	North America	
Miami	25.783	−79.717
Boston	42.367	−70.967
Vancouver	49.200	−123.170
Los Angeles	34.050	−117.767
	Europe	
Madrid	40.260	−3.420
London	51.570	0.280
Athens	38.000	23.380
Moscow	55.450	37.370

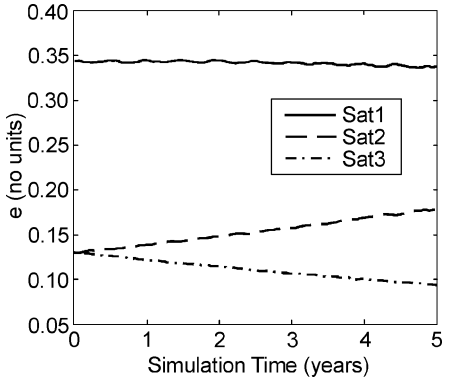

Fig. 4a Five-year propagation: eccentricity.

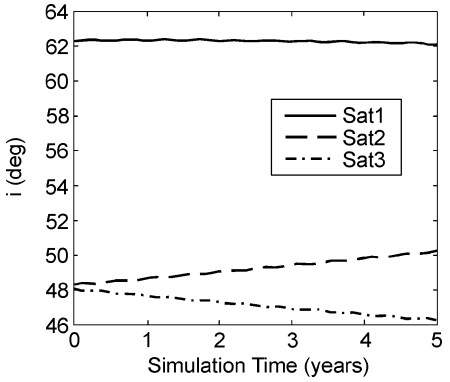

Fig. 4b Five-year propagation: inclination.

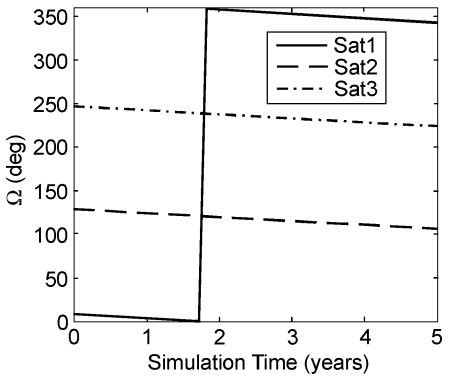

Fig. 4c Five-year propagation: ascending node.

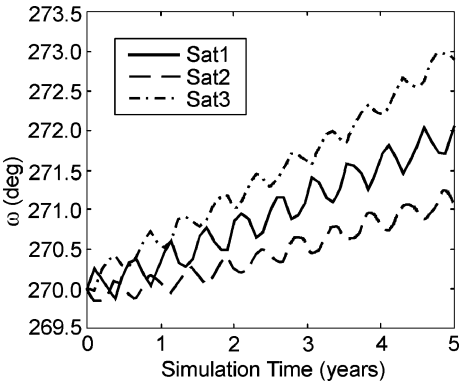

Fig. 4d Five-year propagation: argument of perigee.

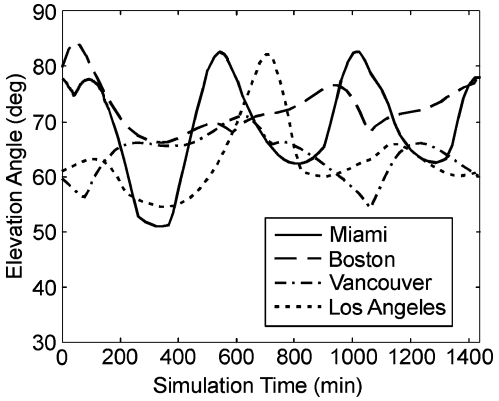

Fig. 5 North American market elevation coverage.

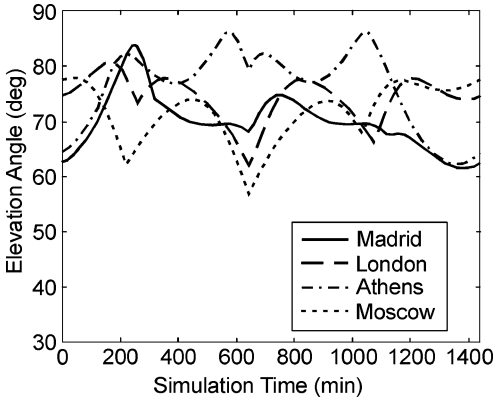

Fig. 6 European market elevation coverage.

constellation were defined with identical mean longitudes. When the argument of perigee equals 270 deg, the ground track can be bisected about the mean satellite longitude, with apogee and perigee located at the mean longitude. Thus, the mean longitude relative to the region of interest can bias coverage east or west. In the case of the North American market, the mean longitude is selected to be 90° west longitude; for the European example, the mean longitude is 17° east. Figures 5 and 6 show the constellation composite maximum elevation angle time history over one day for the various cities.

Figures 5 and 6 show that the goal of 60-deg elevation angle coverage is nearly met. In Fig. 5 there is a region at around 300 min, where the elevation dips fairly low for the two southern-most markets. This region corresponds to when satellite 1 is at apogee. Because this orbit has the highest inclination, the southern-most cities suffer degraded elevation angle coverage as satellite 1 reaches apogee. The other regions of short-term elevation angle coverage correspond to the transition from one satellite providing the highest elevation angles to another.

Stationkeeping

Once a complete constellation has been assembled, its stationkeeping requirements can be evaluated. The primary goal is to maintain the integrity of the constellation and the coverage it provides.

Methodology

It has been observed for Tundra orbits that nearly all of the orbit elements have long period variations that exceed a reasonable tolerance after one year or more. The approach used here is to correct the orbital elements using a traditional "bang-bang" control method. A maneuver interval of once per year was arbitrarily selected. To perform this stationkeeping evaluation, an orbit propagator based in MATLAB® was used. The propagator uses Cowell's method for the long-term prediction of spacecraft behavior subject to perturbations and compares favorably to the POHOP propagator cited earlier. The MATLAB-based propagator is favored for this phase because it allows the necessary stationkeeping algorithms to be built around the propagator. In this way after each propagation period, stationkeeping maneuvers were automatically performed. Following the completion of the maneuvers, the propagation was resumed, and the process was repeated until completion.

The nominal orbits were defined as described in the preceding sections. Each orbit was propagated at one-year intervals for a total of five years. The propagation used a geopotential model of degree eight and order eight (higher-order terms had minimal effects on the results but significantly slowed computational time), solar and lunar gravity. At the conclusion of each propagation period, the need for stationkeeping maneuvers was evaluated. The need for maneuvers was determined by comparing the propagated orbit to the nominal one. If a given element had varied from the nominal value more than its defined tolerance, it was reset to its nominal value using a stationkeeping maneuver.

A Tundra orbit constellation requires the elements Ω, a, and e be controlled precisely to maintain the integrity of the constellation and the cohesiveness of operations. The remaining two parameters, ω and i, are less critical to the actual operations of the constellation and do not need to be maintained as precisely. However, ω and i do impact the quality of the coverage and cannot be ignored. Taking these considerations into account, allowable orbit element deviations are defined such that, when exceeded, a corrective maneuver is deemed necessary.

The tolerances selected for each element are designed to ensure the constellation's integrity. Sample (estimated) values were used in this study. The magnitude of a must be maintained near the synchronous radius in order for the satellite to remain over the desired coverage region; a tolerance of 1 km is used. The eccentricity e must be kept near its design value, or the transition from one satellite to another (as one rises and the other sets) would be adversely affected. The tolerance on e was defined as ± 0.005. This variation on e corresponds to a maximum 4.5-min variation on the time spent in the coverage region and would thus be a total of 9 min for two satellites. The value of ω must also be maintained closely, for as ω increases or decreases the satellite transition is affected, as is the quality of the elevation angle coverage. The tolerance on ω was selected as 1 deg. Inclination is a key parameter in each orbit remaining frozen. The combination of i and Ω define the magnitude of the drift of ω. Because Ω regresses slowly, i is maintained to within 1 deg of the nominal value.

In the case of Ω, a specific value is not the concern, but the relative motion of Ω of all of the satellites must be controlled. For this study, Ω for all satellites is controlled to the mean Ω regression rate of the constellation. The key to this method is to utilize the semimajor axis (i.e., the orbital period) to maintain the satellite's mean longitude rather than a specific ascending node value. Varying the orbital period accordingly allows the satellite to counteract any effect the regressing node has on the mean longitude.

To maintain the broader focus of this study on the overall stationkeeping costs and to simplify the stationkeeping computations, the mean longitude is not maintained. Instead, the initial value of a accounts for both the tesseral harmonic perturbation on semimajor axis[19] as well as the effect of nodal regression. The initial value of a selected results in the mean longitude drifting away from, approximately 6 deg, then back to its initial value during the one-year propagation periods between stationkeeping events. If a tighter tolerance on mean longitude is desired, more frequent maneuvers to adjust the semimajor axis can be performed at a minimal cost.

Once a maneuver is deemed necessary, the required ΔV must be calculated. Meirovitch's formulation[20] expressing changes in orbit elements caused by impulsive maneuvers provides a convenient means by which to compute the ΔV. These changes are given as

$$\Delta a = \frac{2}{n}\left(\Delta V_r \frac{e \sin \nu}{\sqrt{1-e^2}} + \Delta V_t \frac{a}{r}\sqrt{1-e^2}\right) \tag{22}$$

$$\Delta e = \frac{\sqrt{1-e^2}}{na}\left[\Delta V_r \sin \nu + \Delta V_t \frac{a}{er}\left(1 - e^2 - \frac{r^2}{a^2}\right)\right] \tag{23}$$

$$\Delta\omega = -\frac{\sqrt{1-e^2}}{nae}\left\{\Delta V_r \cos\nu - \Delta V_t\left[1+\frac{r}{a(1-e^2)}\right]\sin\nu + \Delta V_n \frac{re\cot i \sin(\omega+\nu)}{a(1-e^2)}\right\} \tag{24}$$

$$\Delta i = \Delta V_n \frac{r\cos(\omega+\nu)}{na^2\sqrt{1-e^2}} \tag{25}$$

$$\Delta\Omega = \Delta V_n \frac{r\sin(\omega+\nu)}{na^2\sqrt{1-e^2}\sin i} \tag{26}$$

where r is the radial distance to the satellite from Earth's center. The impulses are expressed in component form as ΔV_t, ΔV_r, and ΔV_n along the transverse, radial, and orbit normal directions, respectively.

Because most satellites perform maneuvers either normally or transversely within the orbit plane (and not radially), the radial terms are omitted from Eqs. (22–26). Furthermore, because the magnitude of the needed correction to each orbit element is known, the respective required normal or transverse ΔV for each can be determined as follows:

Normal $\Delta V(\Delta V_n)$:

$$\Delta V_n = \Delta i \frac{na^2\sqrt{1-e^2}}{r\cos(\omega+\nu)} \tag{27}$$

$$\Delta V_n = \Delta\Omega \frac{na^2\sqrt{1-e^2}\sin i}{r\sin(\omega+\nu)} \tag{28}$$

$$\Delta V_n = -\Delta\omega \frac{na^2(1-e^2)}{\sqrt{1-e^2}[r\cot i\sin(\omega+\nu)]} \tag{29}$$

Transverse $\Delta V(\Delta V_t)$:

$$\Delta V_t = \Delta a \frac{nr}{2a\sqrt{1-e^2}} \tag{30}$$

$$\Delta V_t = \Delta e \frac{ner}{\sqrt{1-e^2}(1-e^2-r^2/a^2)} \tag{31}$$

$$\Delta V_t = \Delta\omega \frac{nae}{\sqrt{1-e^2}[1+r/a(1-e^2)]\sin\nu} \tag{32}$$

Equations (27–32) show that each element is corrected with either a normal or transverse ΔV maneuver. Because of the nonzero eccentricity, the effectiveness of ΔV_n is affected by the true anomaly of the maneuver. Thus, it is important to specify the location of each maneuver.

Three parameters are affected by ΔV_n: Ω, i, and ω. The large inclination of a Tundra orbit makes correcting ω using ΔV_n inefficient [resulting from the cot(i) term in Eq. (29)]. Therefore, the effect of ΔV_n on ω is not used to find the true anomaly; rather, the (small) change in ω caused by ΔV_n is calculated using Eq. (24) and added to the needed $\Delta\omega$ correction, which is then corrected using the ΔV_t component as described next.

The normal-maneuver true anomaly ν_n is defined as the place where the desired Δi and $\Delta\Omega$ can be achieved simultaneously using one ΔV_n application. This can be determined by setting Eq. (27) equal to Eq. (28) and solving for ν_n, resulting in

$$\nu_n = \arctan\left(\frac{\Delta\Omega\sin i}{\Delta i}\right) - \omega \tag{33}$$

The ΔV_t component is used to correct the elements a, e, and ω. Typically, the ΔV_t required to obtain the needed Δe and $\Delta\omega$ is significantly larger than what is required for Δa. Additionally, when only considering ΔV_t, Δa is affected only slightly by the true anomaly of the maneuver while the semimajor axis increases with a positive ΔV_t and decreases with a negative ΔV_t. Therefore, it is not practical to use a maneuver performed at a single true anomaly because the (single) maneuver needed to correct e and ω would not result in the proper correction to the semimajor axis.

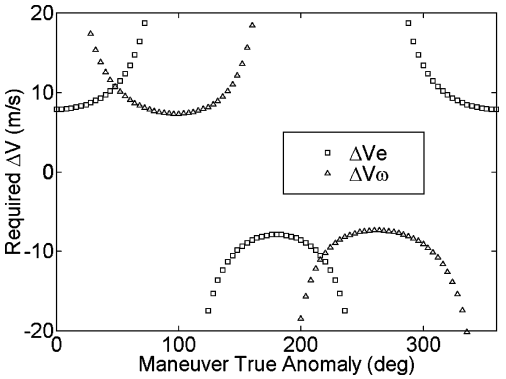

Fig. 7 ΔV_t vs true anomaly.

Equations (31) and (32) are functions of true anomaly and behave like cosecant and secant functions, respectively. Thus, there are two distinct true anomalies at which the desired Δe and $\Delta\omega$ can be achieved for the same ΔV_t. This condition is illustrated in Fig. 7 for an arbitrary Tundra orbit given sample Δe and $\Delta\omega$ values. Because performing all of the required ΔV_t at a single true anomaly will change semimajor axis more than is required, the necessary ΔV_t must be split between the two true anomalies such that the desired Δa is also achieved. The transverse-maneuver true anomalies are determined numerically by stepping true anomaly in small increments (first from 0 to 180 deg then from 180 to 360 deg) and evaluating the ratio of Eqs. (31) and (32). The transverse-maneuver true anomaly is defined where the ratio is nearly equal to one, as illustrated in Fig. 7 by the intersection points that occur twice per orbit.

A similar method is used to determine the amount of ΔV_t that is performed at each true anomaly. A scaling factor F (0–100%) is applied to the first maneuver, performed at the first true anomaly, and the change of orbit elements is calculated. Given the adjusted orbit elements, the second maneuver performs the remaining ΔV_t at the second true anomaly. Because the maneuvers at the two true anomalies are in opposite directions, the semimajor axis is both increased and decreased; summing produces the residual Δa. A simplified algorithm is as follows:

$$\Delta a_1 \sim F\Delta V_t \tag{34}$$

$$\Delta a_2 \sim (1-F)\Delta V_t \tag{35}$$

$$\Delta a = \Delta a_1 + \Delta a_2 \tag{36}$$

If Δa is not close enough to the needed change, F is adjusted, and a new Δa is computed. The loop continues until a value for F is found that achieves the needed correction to the semimajor axis.

When a needed maneuver is computed, the spacecraft velocity state is updated accordingly, and the propagation is resumed using the full model with all perturbations active.

Performance Evaluation

There are two primary metrics considered in assessing the station-keeping methodology: success in maintaining the orbital elements within required tolerances and the amount of ΔV required to maintain them. Figures 8–10 show that a, e, i, and ω were corrected after each one-year propagation period only when their value exceeded their respective tolerance.

It is clearly seen that all of the elements do not require yearly correction. In each plot, the various maneuvers can be seen as the vertical line, or "spike" within the element time history. A spike appearing in only one element and not another is evidence that the maneuver true anomaly corresponds to a position such that only one of the various elements needed to be corrected. Similarly, the large spikes in the semimajor axis history correspond to when eccentricity

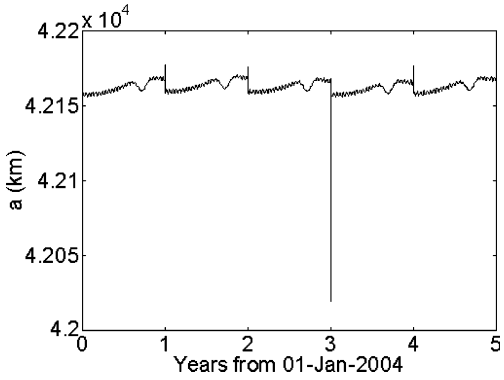

Fig. 8a Satellite 1, orbit maintenance five-year propagation: semimajor axis.

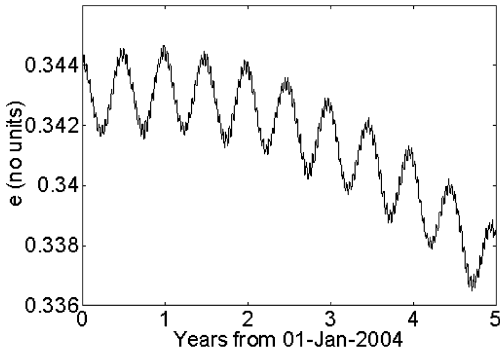

Fig. 8b Satellite 1, orbit maintenance five-year propagation: eccentricity.

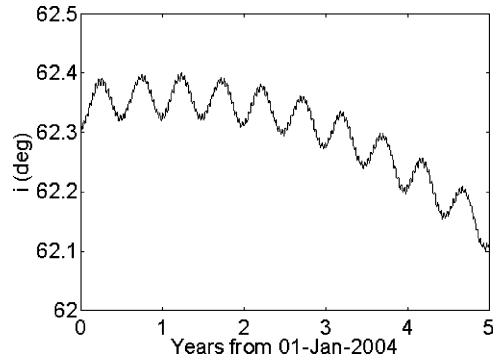

Fig. 8c Satellite 1, orbit maintenance five-year propagation: inclination.

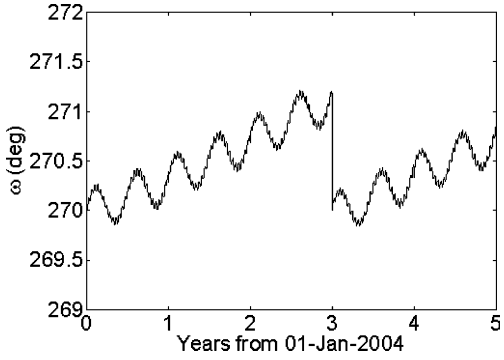

Fig. 8d Satellite 1, orbit maintenance five-year propagation: argument of perigee.

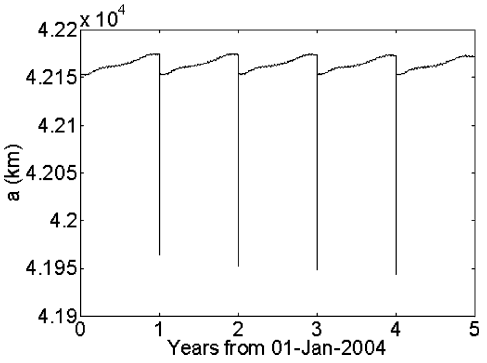

Fig. 9a Satellite 2, orbit maintenance five-year propagation: semimajor axis.

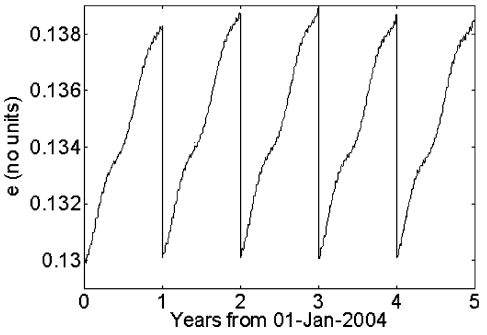

Fig. 9b Satellite 2, orbit maintenance five-year propagation: eccentricity.

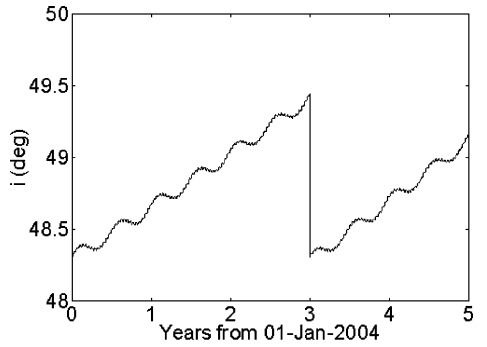

Fig. 9c Satellite 2, orbit maintenance five-year propagation: inclination.

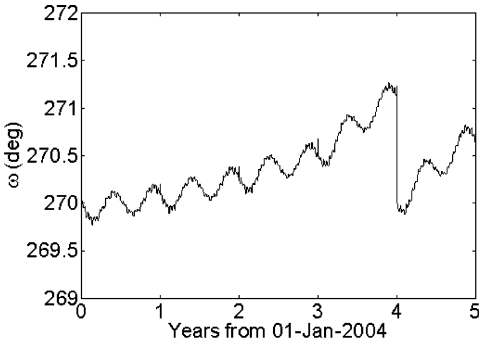

Fig. 9d Satellite 2, orbit maintenance five-year propagation: argument of perigee.

or argument of perigee (or both) were corrected. The algorithm to proportionally split ΔV_t is evidenced by the semimajor axis always being reset to the desired value as well.

Figures 11a–11c illustrate the ascending node variation of each satellite over time with respect to the constellation mean Ω regression rate, 4.67 deg per year. The variation of each orbit's ascending node from the mean is seen as each satellite diverges from zero. A maneuver to adjust the ascending node to correspond to the mean

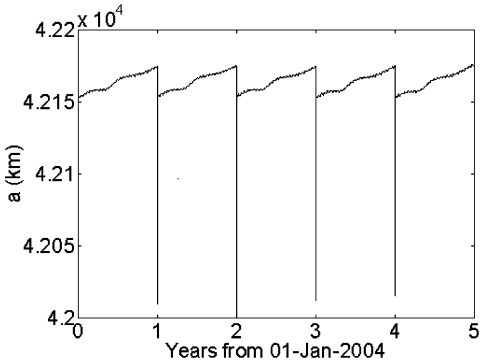

Fig. 10a Satellite 3, orbit maintenance five-year propagation: semimajor axis.

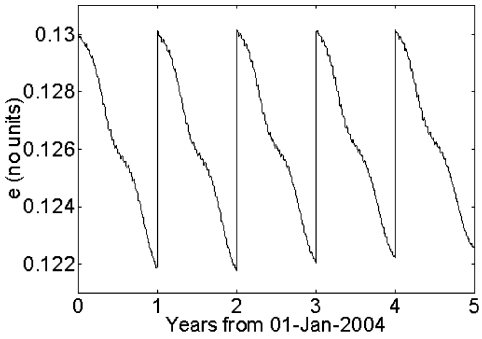

Fig. 10b Satellite 3, orbit maintenance five-year propagation: eccentricity.

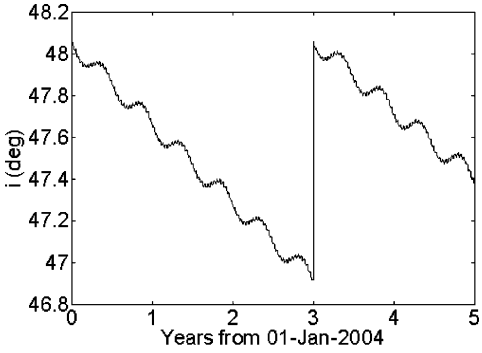

Fig. 10c Satellite 3, orbit maintenance five-year propagation: inclination.

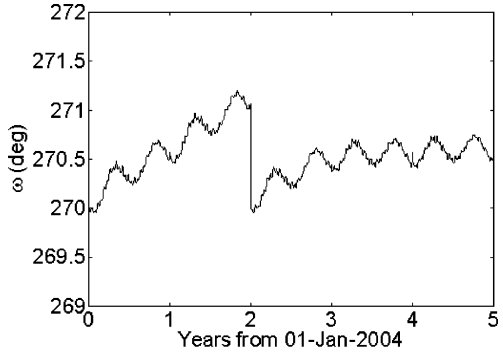

Fig. 10d Satellite 3, orbit maintenance five-year propagation: argument of perigee.

Table 6 Orbit maintenance yearly ΔV frozen constellation

Spacecraft	ΔV_n, m/s	ΔV_t, m/s
Satellite 1	7.2631	4.6052
Satellite 2	18.2506	13.3735
Satellite 3	16.6418	12.5346
Average	14.0518	10.1711

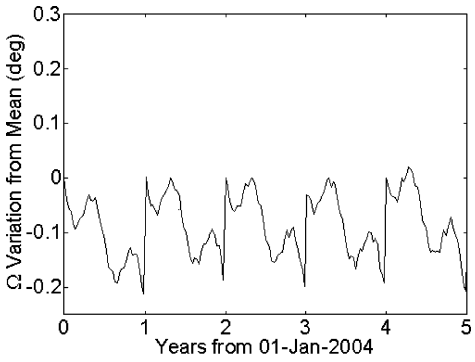

Fig. 11a Satellite 1: Ω correction five-year propagation.

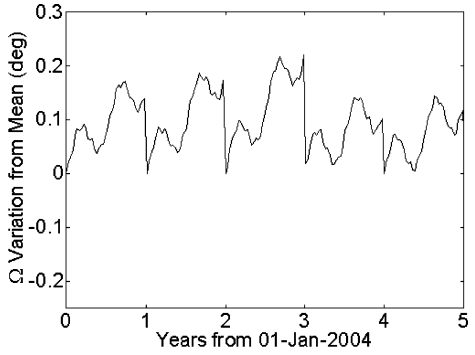

Fig. 11b Satellite 2: Ω correction five-year propagation.

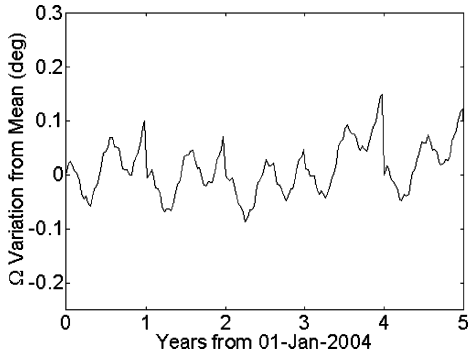

Fig. 11c Satellite 3: Ω correction five-year propagation.

regression rate is similarly represented by the vertical line in the time history. All three orbit planes vary less than a quarter of a degree a year keeping the required corrections small and further helping to reduce ΔV.

The magnitude and frequency of corrections translate directly to required orbit maintenance ΔV. To provide a clearer picture of the true costs over time, the total ΔV was averaged to provide a yearly ΔV requirement. The yearly ΔV requirements directly impact the cost in both mass of the propellant(s) and the propulsion subsystem. The yearly ΔV requirements for each satellite in the constellation are summarized in Table 6.

Table 7 Comparison constellation elements

Element	Sat 1	Sat 2	Sat 3
a, km	42,164.2	42,164.2	42,164.2
i, deg	63.4	63.4	63.4
e	0.2684	0.2684	0.2684
ω, deg	270	270	270
Ω, deg	30	150	270
M,[a] deg	101.02	281.33	185.99

[a]Epoch of 1 January 2004, 00:00 U.T.

Table 8 Orbit maintenance yearly ΔV comparison constellation

Spacecraft	ΔV_n, m/s	ΔV_t, m/s
Satellite 1	29.7365	10.2430
Satellite 2	47.1633	46.4372
Satellite 3	14.4301	36.0858
Average	30.4433	30.9220

As a more meaningful assessment of the constellation design, a comparison baseline (nonfrozen) constellation using the values taken from Table 1 with orbit elements as shown in Table 7 was also used to simulate orbit maintenance requirements.

The values of e and ω of the baseline orbits vary more rapidly over time than those of the frozen constellation resulting in a requirement for yearly correction of both increasing their required ΔV. The required ΔV is further increased because the Ω regression rates between satellites are more varied. Table 8 summarizes the required ΔV for this constellation's maintenance.

It can be seen that there is significant reduction in the required ΔV for orbit maintenance using the frozen constellation. The frozen constellation can reduce ΔV requirements by over 37 m/s per year per spacecraft, on average. The most significant savings occur in the transverse direction. This results from the significant reduction in required ω and e corrections as a result of the frozen nature of the orbits.

Conclusions

The Tundra orbit regime can be a commercially viable alternative to geostationary orbit. These orbits can be made even more desirable by using frozen and nearly frozen orbits as a basis for constellation design. Use of these orbits results in significant reductions in the required orbit maintenance ΔV while nearly achieving the desired coverage goals. These savings can be returned to the operator in the form of lower procurement and operating costs.

Nearly frozen orbits in the Tundra regime have been identified and can be of use to future mission designers. A constellation designed with such orbits provides an operator with significant propellant savings over the lifetime of the constellation and thus significant cost savings. The method for searching for frozen orbits described here uses a doubly averaged perturbation model in identifying useful Tundra orbits. Adaptation of the frozen orbit search allows the discovery of partially frozen or nearly frozen orbits with which a complete constellation can be designed. Future efforts will attempt to "better" freeze the orbits by selecting elements that minimize drift over time (instead of at the initial time only).

This study examined only one Tundra constellation configuration. Although significant orbit maintenance benefits are shown, the coverage limitations of the three-satellite constellation and the limits on the allowable orbit elements are also exhibited. The quality of coverage could be improved either by increasing the minimum allowable eccentricity or by adding additional satellites to the constellation. Increasing the minimum eccentricity would ensure a greater percentage of time spent in the hemisphere of interest. This would likely come at a relatively small cost in additional ΔV relative to the baseline constellation. Similarly, the coverage could also be improved by the addition of one or more satellites. Finally, examination of how much drift can be tolerated in various elements (RAAN in particular) will be a topic of future study.

References

[1]Davies, J. K., *Space Exploration*, W&R Chambers, Ltd., New York, 1992, p. 36.

[2]Briskman, R. D., and Nelson, R. A., U.S. Patent No. 6,223,019, 24 April 2001.

[3]Barker, L., and Stoen, J., "Sirius Satellite Design: The Challenges of the Tundra Orbit in Commercial Spacecraft Design," *Advances in the Astronautical Sciences*, Vol. 107, 2001, pp. 575–596.

[4]Turner, A. E., "Molniya/Tundra Orbit Constellation Considerations for Commercial Applications," American Astronautical Society, AAS Paper 01-215, Feb. 2001.

[5]Draim, J. E., Inciardi, R., Proulx, R., Cefola, P., Carter, D., and Larsen, D. E., "Beyond GEO—Using Elliptical Orbit Constellations to Multiply the Space Real Estate," *Acta Astronautica*, Vol. 51, Nos. 1–9, 2002, pp. 467–489.

[6]Cefola, P., Draim, J. E., Inciardi, R., Proulx, R. J., and Carter, D. W., "The Orbital Perturbation Environment for the COBRA and COBRA Teardrop Elliptical Constellations," American Astronautical Society, AAS Paper 02-173, Jan. 2002.

[7]Dufour, F., "Optimal Continuous Coverage of the Northern Hemisphere with Elliptical Satellite Constellations," American Astronautical Society, AAS Paper 04-110, Feb. 2004.

[8]Mass, J., and Sartiel, J., "Orbits for Earth Observation," *Collection of Papers of the 26th Israel Annual Conference on Aviation and Astronautics*, Israel Inst. of Technology, Tel-Aviv, Israel, 1984, pp. 179–194.

[9]Rondinelli, G., Cramarossa, A., and Graziani, F., "Orbit Control Strategy for a Constellation of Three Satellites in Tundra Orbits," American Astronautical Society, AAS Paper 89-411, Aug. 1989.

[10]Rosborough, G., and Ocampo, C., "Influence of Higher Degree Zonals on the Frozen Orbit Geometry," *Advances in the Astronautical Sciences*, Vol. 76, Pt. 2, 1992, pp. 1291–1304.

[11]Coffey, S. L., Deprit, A., and Deprit, E., "Frozen Orbits for Satellites Close to an Earth-Like Planet," *Celestial Mechanics and Dynamical Astronomy*, Vol. 59, No. 1, 1994, pp. 37–72.

[12]Bruno, M. J., "Tundra Constellation Design and Stationkeeping," M.S. Thesis, Dept. of Mechanical and Aerospace Engineering, San José State Univ., San José, CA, Dec. 2003.

[13]Bruno, M., and Pernicka, H., "Mission Design Considerations for the Tundra Constellation," AIAA Paper 2002-4634, Aug. 2002.

[14]Broucke, R. A., "Long-Term Third-Body Effects via Double Averaging," *Journal of Guidance, Control, and Dynamics*, Vol. 26, No. 1, 2003, pp. 27–32.

[15]Cefola, P., "Long-Term Evolution of Near-Geostationary Orbits—Comment," *Journal of Guidance, Control, and Dynamics*, Vol. 10, No. 2, 2003, pp. 222, 223.

[16]Kwok, J. H., "A Doubly Averaging Method for Third Body Perturbations in Planet Equator Coordinates," American Astronautical Society, AAS Paper 91-464, Aug. 1991.

[17]Larson, W. J., and Wertz, J. J., *Space Mission Analysis and Design*, 2nd ed., Microcosm, Inc., Torrance, CA, 1993, pp. 199–201.

[18]Press, W. H., Flannery, B. P., Teukolsky, S. A., and Vetterling, W. T., *Numerical Methods: The Art of Scientific Computing*, Cambridge Univ. Press, Cambridge, England, U.K., 1986, pp. 283–286.

[19]Soop, E. M., "Introduction to Geostationary Orbits," ESA, SP-1053, Paris, Nov. 1983.

[20]Meriovitch, L., *Methods of Analytical Dynamics*, McGraw–Hill, New York, 1970, p. 456.

C. McLaughlin
Associate Editor